Expanding the scope of fast timing photo-detection with the more affordable, second generation LAPPD^{TM}

Evan Angelico, Andrey Elagin, Henry Frisch, Todd Seiss, Eric Spieglan

Enrico Fermi Institute, University of Chicago, United States

Bernhard Adams

Incom, Inc. 294 Southbridge Road, Charlton, MA 01507

Abstract

A broad range of physics applications (neutrino detector physics, time projection chambers, collider physics, medical imaging) have proposed the use of fast timing photo-multipliers. These applications only scratch the surface. The goal of the LAPPD project is to enable affordable fast timing measurements in physics. The Large-Area Picosecond Photo-Detector (LAPPD^{TM}) is a planar, 20×20 cm^2 photo-multiplier that is being developed for sub-pico second timing resolution and large area detector coverage. The first generation LAPPD^{TM} uses transmission line anode strips to carry signals from the inside of the vacuum volume to external electronics. A second generation LAPPD has been proposed to reduce manufacturing costs while maintaining timing capabilities. The Inside-Out LAPPD uses a thin metal ground plane inside the vacuum volume that capacitively couples to a readout board outside of the vacuum volume. Two inside-out anode candidates were tested: a large, square 10nm NiCr film, and a 1kΩ per square resistive film. The two inside-out anodes retained 31.4% and 35.8% of the MCP signal respectively. This experiment has proven that it is possible to extract MCP signals through a ceramic vacuum wall while maintaining pico-second rise times, marking a new step towards affordable fast timing technology.

Keywords:
photo-detector, photo-multiplier tube (PMT), fast timing, micro-channel plate (MCP), Large Area Pico-Second Photo-detector (LAPPD), picosecond

Contents

1 Introduction **3**
- 1.1 Applications of fast timing and precise position resolution . . . 3
  - 1.1.1 Neutrino Physics . . . 4
  - 1.1.2 Positron emission tomography (PET) . . . 5
- 1.2 Present status . . . 5
  - 1.2.1 Generation I LAPPD . . . 6
  - 1.2.2 Generation II - motivation . . . 8

2 The Inside Out **11**
- 2.1 Approach . . . 11
- 2.2 Benefits . . . 11
- 2.3 Circuit diagram . . . 11
- 2.4 Test inside-out (IO) anodes . . . 12
- 2.5 Strip-line vs pads . . . 14

3 Experimental setup **14**
- 3.1 Test apparatus . . . 14
- 3.2 Signal amplitude on direct strip-lines . . . 15
- 3.3 Systematic error . . . 15

4 Measurements of signal amplitude **15**
- 4.1 Typical pulses . . . 15
- 4.2 Signal amplitude on inside-out anode . . . 16
- 4.3 Rise time comparison . . . 17

5 Results and discussion **20**

6 Conclusion **20**

7 Acknowledgments **20**

1. Introduction

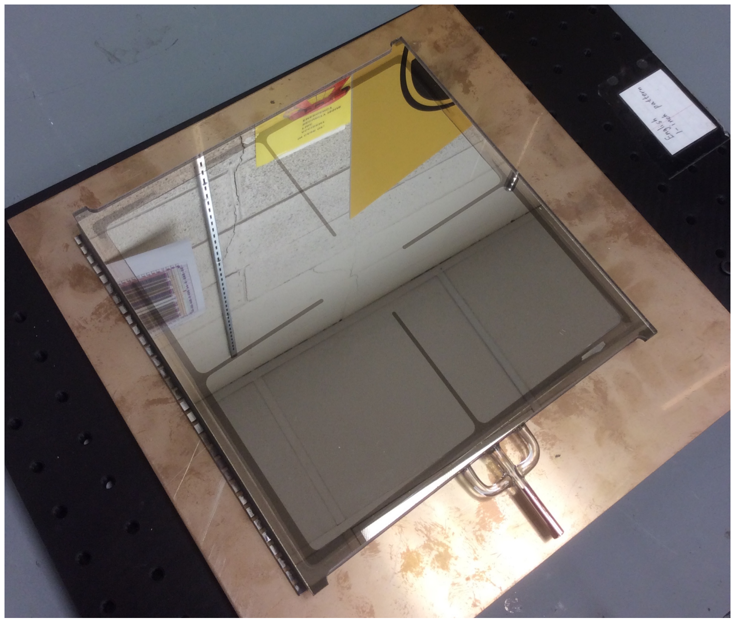

Figure 1: Top-down view of a sealed, LAPPD photo-detector "tile" made by the team at University of Chicago. The reflective surface is 20nm thick antimony used as a substrate for the photo-cathode (this tile has no photocathode yet). The LAPPD is under vacuum when measuring photo-signals. The silver anode strip-lines, which carry a charged photo-signal, are peeking out from the vacuum packaging.

1.1. Applications of fast timing and precise position resolution

Conventional photo-multiplier tubes have time resolution of at best $\sim$ 1ns [1]. Micro-channel plate (MCP) photo-detectors are in commercial use, and can provide timing resolutions of as low as $\sim$ 30 pico-seconds [1]. But measurements of 10^{-12}s are only scratching the surface of a vast degree of new physics at small time scales. Average chemical reactions are on the order of 500fs, and heavy boson decays are the order of 10^{-25}s [2]. There is no reason not to push for detection technologies which can explore these timescales.

The pico-second timing regime is accessible through the MCP photo-detector technologies currently available on the market. A detector with 25cm^2 area is roughly $11,000. The high price per square cm of detection area makes pico-second measurements unrealistic in large physics experiments which have to cover tens of thousands of square meters with photo-detectors.

The following are a few proposed applications of fast timing in physics:

1.1.1. Neutrino Physics

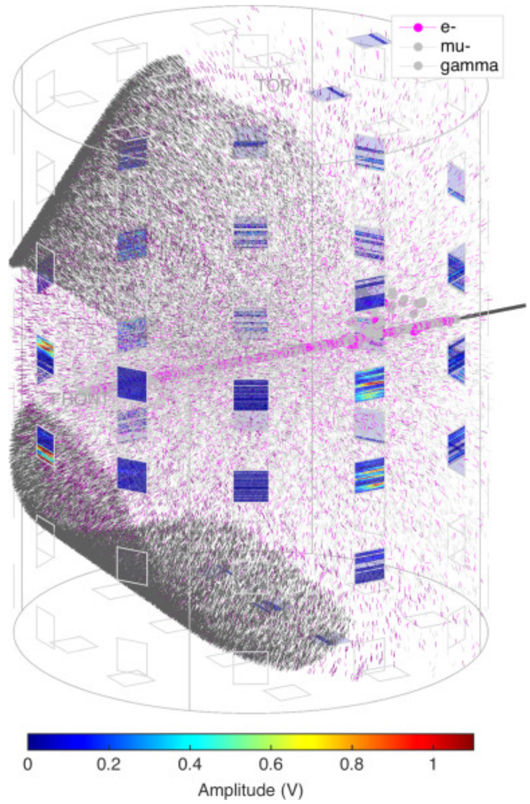

Figure 2: Figure 9. from reference [3]. Simulated event display for a 10 GeV muon traversing the ANNIE [4] water Cherenkov detector. The image is capture 12ns after the muon enters the detector. About 2500 PEs are collected over the 96 ANNIE LAPPDs per muon event.

A water-Cherenkov detector, called The Accelerator Neutrino Neutron Interaction Experiment (ANNIE) is being deployed at the Fermilab beam line [4]. ANNIE intends to tag the presence of all neutrons which appear in decays within a large volume of Gadalinium doped water. ANNIE can play a significant role in reducing the atmospheric neutrino backgrounds of water based neutrino experiments by measuring the number of neutrons produced in neutrino interactions as a function of momentum transfer. In particular, proton decay experiments rely on measuring the existence *and* non-existence of short lived neutrons resulting from weak decays. ANNIE plans to use precision timing to localize interaction vertices in the small fiducial volume of the detector. A large area micro-channel plate photo-multiplier can provide the timing necessary for ANNIE's measurements.

Eric Oberla recently used commercial MCP photo-multipliers to track relativistic charged particles by 'drifting' Cherenkov photons in a water-based time projection chamber. The Optical Time Projection Chamber (OTPC) was able to reconstruct 3 + 1 dimensional tracks created by particles in the Fermilab test beam by measuring time differences of $\lesssim$ 50ps [5] in the arrival of Cherenkov photons traveling in water. Most time projection chambers drift electrons in purified gases or expensive materials [6]. With fast timing, Eric was able to drift photons in a cheap detection medium: water.

Cherenkov light is present in liquid scintillator, but is overlooked in neutrino experiments because the high intensity of scintillation light washes out Cherenkov light [7]. In most media, however, Cherenkov light occurs earlier and travels faster than scintillation light [7]. Fast timing photo-detectors have the ability to separate Cherenkov light from scintillation light, thereby extracting directionality information of particle interactions and retaining the useful information provided by the scintillation light. [8]

1.1.2. Positron emission tomography (PET)

Positron Emission Tomography (PET) is a medical imaging module used to locate radioactive-tracer in organs with high metabolic activity [9, 10, 11]. The radioactive tracer material emits a positron which annihilates with an electron producing roughly back to back photons. The photons arrive at a scintillator, creating a light shower measured by photo-multiplier tubes or silicon photodiodes. The vertex of the annihilation is reconstructed using the Time-of-Flight of the initial photons. [9]

Using MCP photo-multipliers and fast timing, PET scanners could use the Cherenkov light produced in water to detect the tracer. Large area MCP photodetectors would reduce the cost PMTs in a PET scanner, remove the need for scintillator, and improve vertex position reconstruction. [9]

1.2. Present status

The LAPPD collaboration has developed an MCP photo-multiplier with 16 times the area of the present commercial model. The University of Chicago and others [12] are attempting to manufacture large quantities of LAPPDs at prices which are affordable to the vast majority of physics applications. Currently, the process design and detector design is too expensive to compete with the conventional high performance PMT.

1.2.1. Generation I LAPPD

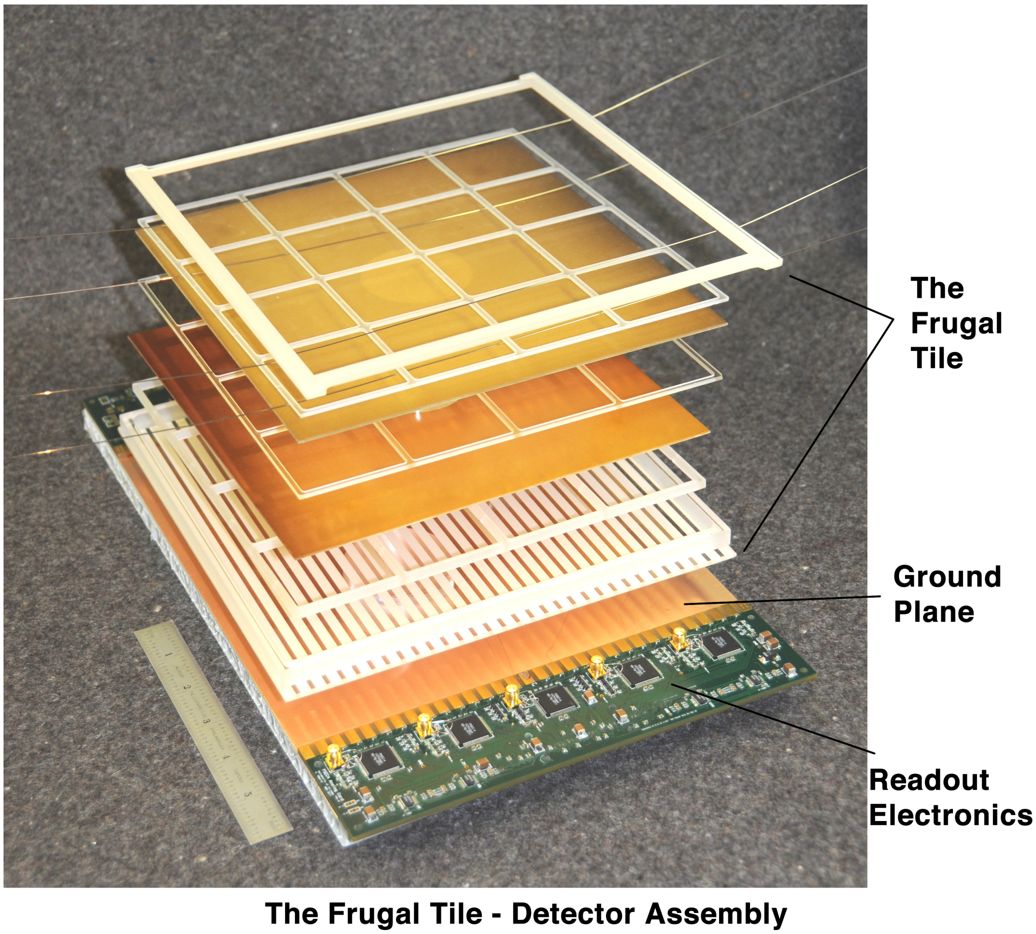

Figure 3: The first generation, 'Frugal Tile' assembly. From top down: top photo-cathode window, two MCPs separated by spacers, sidewall and anode lower tile assembly, ground plane, electrical readout.

The Large-Area Picosecond Photo-detector (LAPPD^{TM}) is a planar, 20×20 cm^2 photo-multiplier tube that is being developed for sub-picosecond timing resolution and large area detector coverage.

The first generation LAPPD consists of (see Figure 3) a top window with deposited photo-cathode material, a stack of two MCPs separated by resistive spacers, and a lower tile base with micron thick silver strip-lines traversing the 20cm length.

The LAPPD is itself a high voltage divider. High voltage is applied across the anode (strip-line tile base) and the cathode (photo-cathode top window), and DC current flows through a chain of MΩ restive spacers and MCPs (see Figure 6a).

The photo-multiplication process of an LAPPD is similar to that of a conventional photo-multiplier tube. In a PMT, a primary electron born at the photo-cathode is accelerated towards metal plates called dynodes. The dynodes emit secondary electrons, and a chain of dynodes creates an electron avalanche.

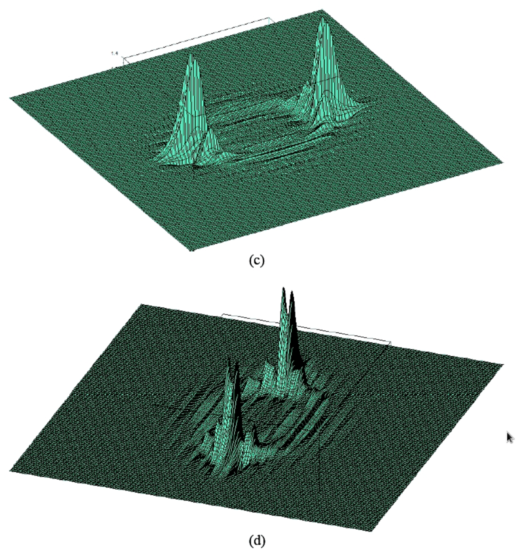

Figure 4: This figure from [13] shows a simulated pulse amplitude propagating on the strip-line anode. Both pictures have 30 strips in the plane. The primary pulse is shared among neighboring strips.

An LAPPD uses two MCPs as a continuous dynode stage for electron multiplication. Micro-pores are glass capillary channels for which the electrons can undergo secondary emission. With millions of micro-pores, a single primary electron can multiply to a gain of 10^7 [12]. A uniform electric field is maintained across the MCPs that accelerates electrons toward the anode plane.

The anode consists of a set of parallel transmission lines, or "strips" (Figure 5a). The MCPs deliver a charge shower to the strips inducing two pulses which propagate in opposite directions (see simulated visualization, Figure 4 [13].

The pulses are recorded by electronic readout cards connected to the ends of the strip-lines. The difference in arrival time between the two propagating components determines the incident photon position and arrival time along the anode. Signals are measured by a 10.24GSPS digitizer called PSEC4 (see section 3).

1.2.2. Generation II - motivation

The goal of the LAPPD project is to have an affordable detector with picosecond timing resolution or better. The cost of a single LAPPD increases with the time that it takes to fabricate. Therefore, to reduce the cost of an LAPPD, the fabrication process must be simple and seamless.

The proposed second generation LAPPD attempts to make cost saving simplifications to the manufacturing process while maintaining fast timing characteristics.

The second generation LAPPD:

1. Replaces the glass packaging with a higher bandwidth ceramic packaging
    - The dielectric loss tangent of alumina ceramic is almost an order of magnitude lower than glass [1]. A detector made of alumina ceramic has better analog bandwidth, and is thus has better timing characteristics.
    - High fire alumina ceramic is more robust[2] than glass, is more difficult to shatter during fabrication, and can be heated to > 800C.
2. Splits the anode into two separate entities, the internal anode and the external readout board
    - In place of the first generation anode is a homogeneous thin metal film. This is easier to manufacture and more robust than the strip-line anode.
    - The readout board sits outside of the LAPPD packaging, coupling to the internal ground plane capacitively.
    - Having two separate entities for the anode and the readout allows for the readout pattern to be customized and optimized, while the LAPPD design stays fixed.

[1]First generation LAPPDs use Borofloat 33

[2]During this experiment, we found that the commercial MCP photo-detectors are delicate and easily broken. Having a robust design is critical for deploying mass quantities of LAPPDs.

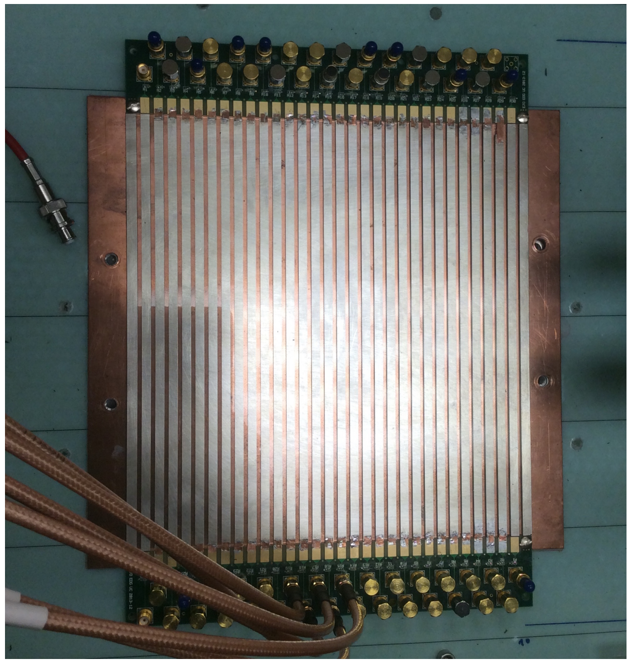

(a) This is a strip-line anode repurposed as a readout board for inside-out testing. The strip-lines capacitively pick up an inside-out signal and transmit that signal to digitizing electronics.

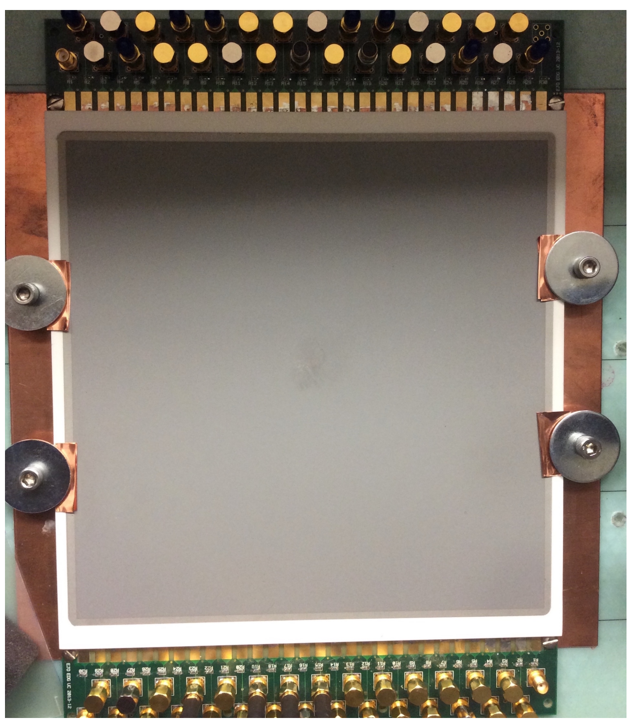

(b) Here is an inside-out anode made of 10nm NiCr thin film, with a ticker NiCr ground boarder. The homogeneous metal layer is deposited on the ceramic tile base (the second generation LAPPD is made of ceramic instead of glass). The strip-line readout is below the ceramic base. The NiCr layer capacitively couples to the strip-lines below and induces a signal.

Figure 5

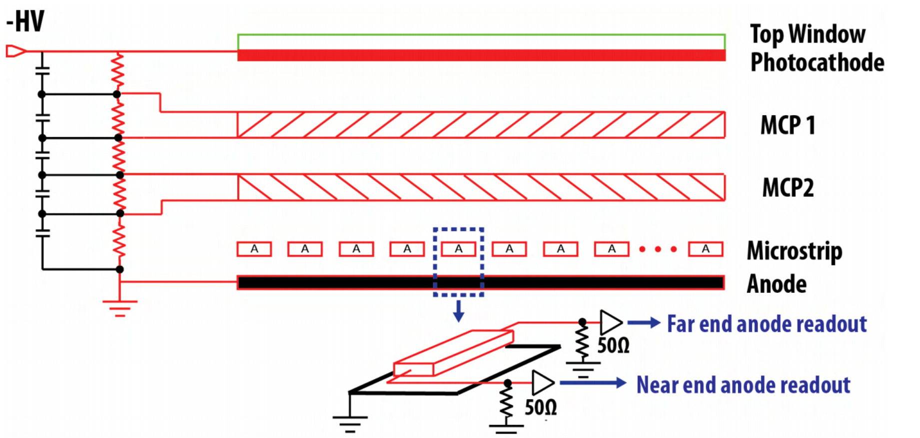

(a) A circuit schematic of the first generation LAPPD. The MCPs and air gaps act as resistances and capacitances in series, forming a high voltage divider between the photo-cathode and anode. The anode strips, that are internal to the vacuum volume, receive charge shower signals read out differentially by electronics external to the vacuum volume.

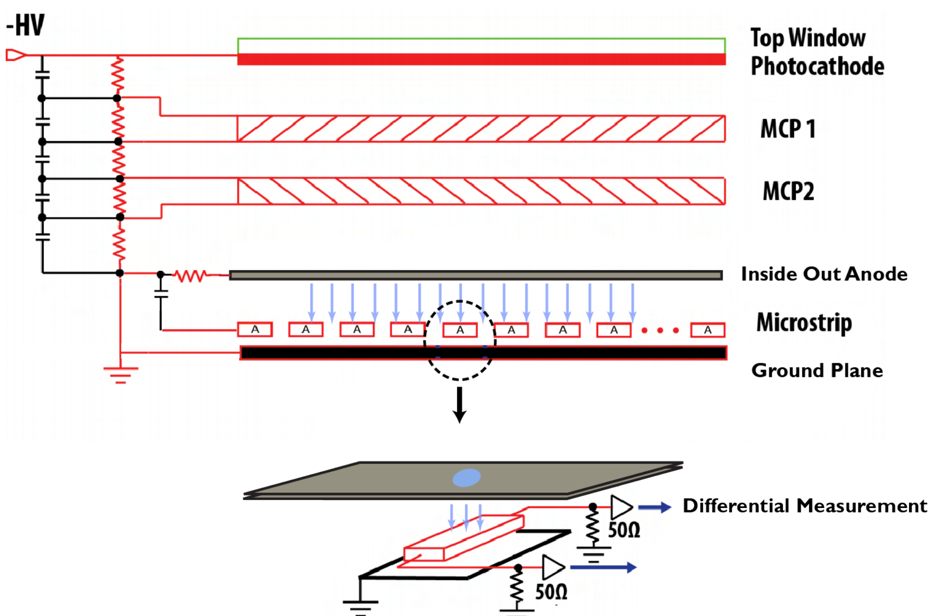

(b) The second generation, Inside-Out LAPPD schematic. The anode is a large, thin metal ground plane instead of discrete strip-lines. On the outside of the vacuum volume, a readout pad pattern (or strip-line pattern) capacitively couples to the anode inside the vacuum volume. The induced signal is read out differentially on the readout pattern.

Figure 6

These two changes both decrease the cost of manufacturing, and maintain (if not improve) the timing characteristics of the LAPPD.

2. The Inside Out

In the second generation LAPPD, the anode has been separated into two entities: the inside-out anode and the readout board. This experiment focuses on testing the transmission properties of the inside-out anode, which is internal to the detector.

2.1. Approach

The *Inside-Out* anode anode is a homogeneous metal ground plane deposited on an LAPPD ceramic base plate (Figure 5b). It receives charge showers from the MCPs. The readout board, which sits flush to the base of the LAPPD, capacitively couples to the inside-out anode. Signals are extracted from the readout board. Therefore, no electrical connections are made to the inside-out anode which lies internal to the LAPPD vacuum volume.

2.2. Benefits

The inside-out anode, being a homogeneous thin metal film, is less costly to fabricate than the strip-line anode. Reducing the cost of parts (and the time it takes to make those parts) puts us one step closer to an affordable device.

The readout board is completely separate from the LAPPD photo-detector, and can be optimized independently for application specific needs. No matter what readout pattern is desired, the user buys one design of LAPPD which means less parts to consider during manufacturing.

We have seen that our micron thin silver strips evaporate at low enough temperatures to become relevant during fabrication. Removing the silver strips from inside of the LAPPD allows for a wider range of temperatures. The silver strips can instead be on the readout board, which is a separate item.

2.3. Circuit diagram

The inside-out anode forms an RC circuit with the readout board. An effective circuit diagram is shown in Figure 7.

The effective circuit is an *RC* high-pass filter. The fast LAPPD signal is measured differentially from the readout board. The cutoff frequency is

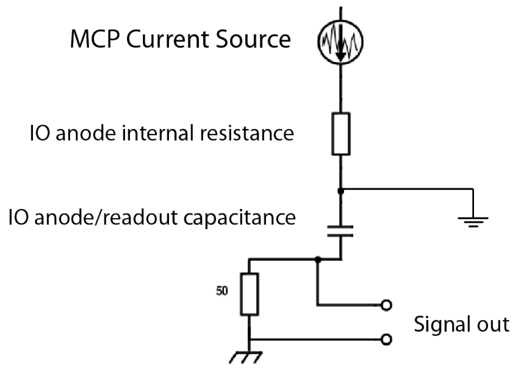

Figure 7: Circuit schematic of an AC inside-out LAPPD. The end of the MCP stack acts as an RF current source. The signal couples to the readout (labeled signal out) through the RC filter. The 'capacitor' is a parallel plate: one plate is the inside-out anode, one plate is the readout board.

$$\omega_c = \frac{1}{RC} \tag{1}$$

where C is the capacitance of the inside-out anode and the readout board, and R is the internal resistance of the inside-out anode. To allow pico-second rise time pulses through the capacitance, ω_c must be less than 1GHz.

To increase the product, RC, we may increase the resistivity and decrease the thickness of the inside-out anode.

The semi-conductor industry has developed a method for depositing large areas of resistive ink that has a tuneable "resistance per square" [14].

Figure 8 shows the cutoff frequency as a function of (top) resistance per square, and (bottom) thickness of common evaporable metal.

2.4. Test inside-out (IO) anodes

Based on this calculation, two test anodes were chosen for the present experiment as plausible inside-out anodes candidates:

- 10nm thin film NiCr on a 3mm alumina ceramic substrate: $\sim$ 100Ω per square resistance
- Resistive ink fired onto a 3mm alumina ceramic substrate: $\sim$ 1kΩ per square resistance

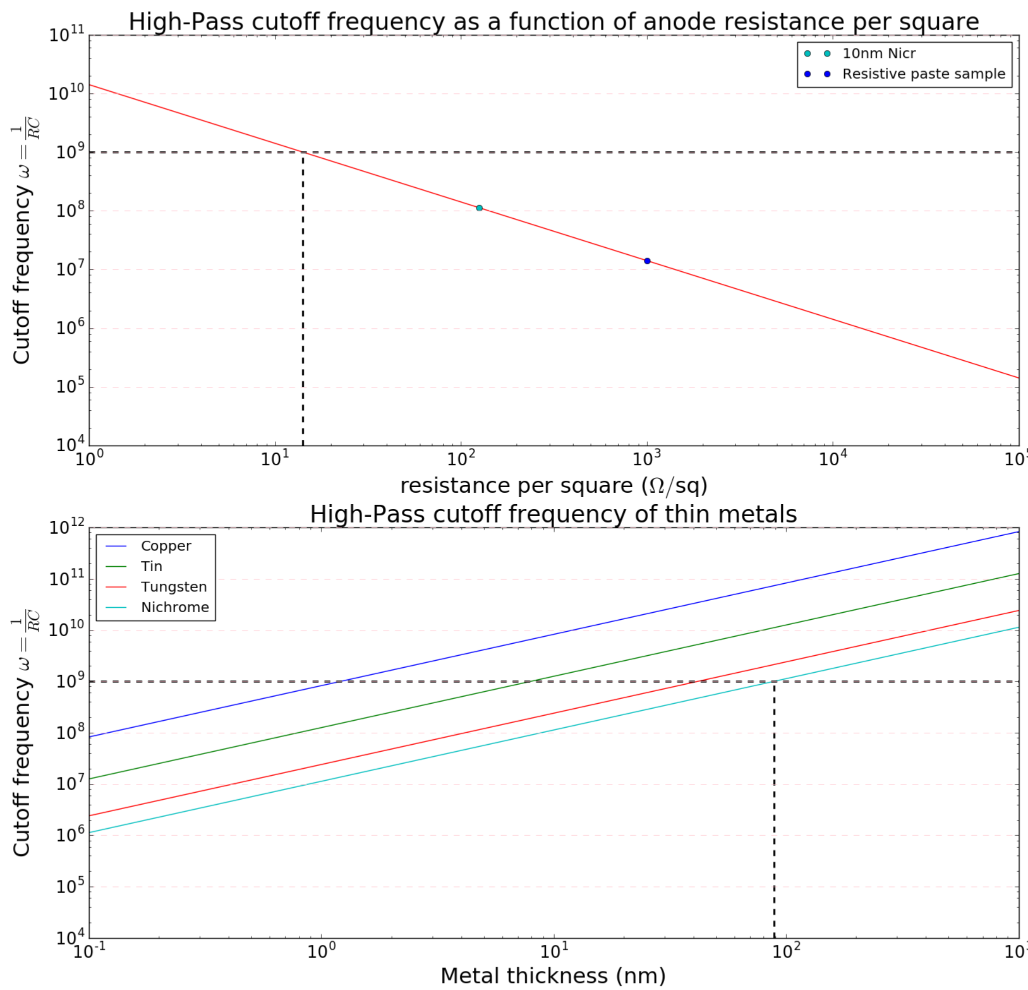

Figure 8: The above plots show the result of treating the inside-out anode/readout system as an RC high pass filter. (TOP) Shows that an inside-out anode with tunable resistance per square must be more resistive than $\sim 20\Omega$ per square for $\omega_c < 1$GHz. Blue and cyan points indicate the resistance per square and cutoff frequency of the presently tested inside-out anodes. (BOTTOM) Shows cuttoff frequency as a function of metal thickness for four common evaporable metals. Both of these calculations assume an anode area of $20 \times 20\text{cm}^2$, separated from the readout board by 3mm thick ceramic of dielectric constant $\epsilon_r = 9$

The NiCr sample was evaporated by collaborators at Incom and Argonne National Labs (ANL) [15], and the resistive ink sample was fabricated by the company Hybrid-Tek [14].

2.5. Strip-line vs pads

The strip-line readout pattern is optimized for high analog bandwidth to provide position resolution of $\sim$ 700 microns [12]. The arrival time of events on a strip line is determined by the difference in arrival times of pulses. Therefore, the strip-line readout pattern has the highest position resolution, but is incapable of operating in high occupancy environments.

Todd Seiss is exploring the consequences of using a pad pattern readout for an LAPPD [16]. The pad pattern does not have optimized analog bandwidth, and sacrifices position resolution in return for high occupancy readout.

This experiment uses a strip-line readout pattern because of its high analog bandwidth and its ability to directly compare to the first generation LAPPD. The strip-lines provide the best position resolution and have been proven to transmit LAPPD signals. The same strip-line anodes are used in the first-generation LAPPD. Therefore, by using strip-lines as a readout pattern, a direct comparison can be made between inside-out LAPPDs and first generation LAPPDs.

3. Experimental setup

3.1. Test apparatus

LAPPD-like pulses are replicated with a commercial MCP photo-multiplier. The "Planacon" XP85022 MCP-PMT device from PHOTONIS has a $5\times5\text{cm}^2$ active photo-detection area. Its anode consists of a 32×32 pad array which, in normal operation, are bonded to a PCB readout card with a low temperature cureable silver epoxy [17].

Planacon pulses are known to have slower rise times and lower amplitude signals compared to a prototype LAPPD [3, 17]. If the inside-out anode transmits Planacon pulses, then the inside-out anode will transmit LAPPD pulses at the same or higher signal to noise ratio.

The light source is a 405 nm diode laser from Advanced Laser Systems [18]. The laser is operated in pulsed mode, with durations of 33ps and pulse rates between 100Hz and 1MHz. A single mode fiber coupling allows for positional scans of the laser over the active area of the Planacon. In this experiment, pulse rates of 100Hz are used.

Signals are digitized with a PSEC4 ASIC evaluation card [19]. This is a custom, compact, six-channel oscilloscope designed by Eric Oberla at University of Chicago. PSEC4 has a 10.24GSPS sampling rate and 10.5 bit effective precision. The electronics are triggered with the laser pulse, and the 25 ns buffer depth of PSEC4 captures the full extent of the Planacon signal.

In the control setup, the Planacon sits directly on strip-lines read out by PSEC4. In the inside-out setup, an inside-out anode is placed in between the Planacon and the readout board. The strip-line readout board capacitively couples to the inside-out anode and is read out by PSEC4.

3.2. Signal amplitude on direct strip-lines

Signal amplitude is used as a figure of merit for LAPPD performance. S. Ritt [20] showed that the timing resolution of an LAPPD may be calculated, and is proportional to $\frac{\Delta U}{U}$, where U is the signal amplitude. We expect some degree of amplitude loss when switching to an inside-out anode. The a pure loss in amplitude from inside-out is directly related to a loss in timing resolution.

3.3. Systematic error

A systematic error of 50mV is placed on all amplitude measurements, due to an inconsistent electrical connection to the Planacon. In normal operation, all 1024 anode pads of the Planacon must be terminated to ensure that charge does not build up inside the photo-tube. The consequence of not terminating the anode pads is a loss in signal amplitude.[3] In this experiment, $4 - 16$ anode pads are terminated to the strip-lines by a small dot of uncured silver epoxy. The number of pads that make contact with the silver epoxy dramatically affects the amplitude of the measured signal. The procedure followed intends to use a consistent volume of silver epoxy. Through repeated placement of the Planacon, we have estimated a systematic error of 50 mV on the amplitude of the center strip-line signal.

4. Measurements of signal amplitude

4.1. Typical pulses

A typical event on all channels, and on the main channel, is shown in Figure 9. The signal amplitude is defined as the absolute maximum value of the pulse.

This test will present measurements on the main channel only, i.e. the channel directly below the laser/silver dot. The majority of the signal is contained on the main strip (nearest neighbor has $\sim$ 10% of main strip amplitude). Todd Seiss [16] discusses how cross talk between channels affects event reconstruction.

[3] A charged anode sits at a higher potential relative to the nearest MCP. Therefore, electrons arrive at the anode with less energy. Some fraction of these electrons will not discharge, thus lowering the signal amplitude.

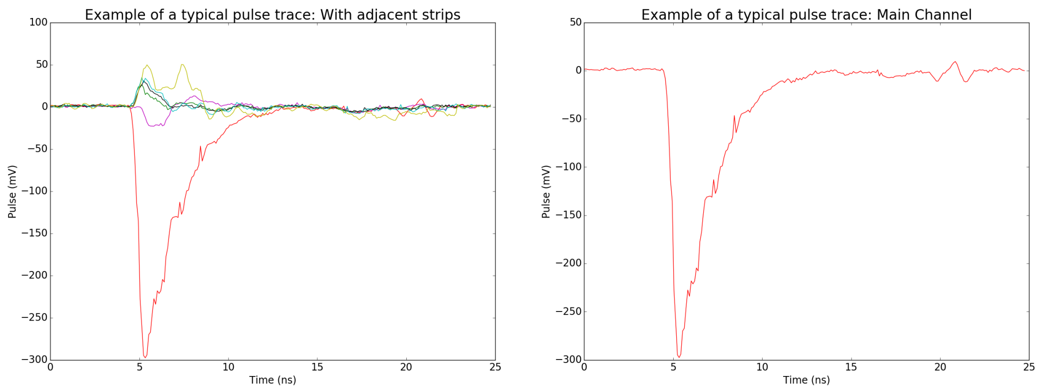

Figure 9: On the left is a typical event, with all six channels plotted. The channels with smaller amplitude are neighbors of the center strip-line, shown in red on both plots. Signals in the other channels arise due to mutual capacitances between neighboring strips. The figure on the right is the main pulse on the center strip-line. The center strip (or main strip) is the focus of this paper.

4.2. Signal amplitude on inside-out anode

In this experiment, two samples are tested as inside-out anodes: a 10nm NiCr thin film and a 1kΩ per square resistive ink, both on a 3mm thick ceramic anode base.

The inside-out test anode is inserted between the Planacon and strip-line readout. The laser head and silver epoxy dot is placed on top of the inside-out anode, in the same position as in the direct measurement setup: directly above the center strip-line. The only difference between the direct setup and the inside-out setup is that the Planacon signal lands on the inside-out anode instead of directly on the strip-line readout board.

Figure 10 compares a single pulse on both the inside-out and direct setup. Notice that the low frequency features in the direct pulse (around 20ns) are also seen in the inside-out anode setup. This suggests that the mutual capacitances in the direct setup are consistent with those in the inside-out setup.

Figure 11a shows the average signal amplitude at various applied high voltages for direct strip-line, NiCr, and Ink inside-out samples. Error bars represent both the 50mV systematic error and a small, $\lesssim$ 1mV statistical error.

Figure 11b plots the constant ratio of amplitudes between the inside-out anodes and the direct strip-line measurement. The standard deviation of this ratio with respect to applied HV is 0.7% in both inside-out samples. The 50mV systematic error from making the electrical connection to the Planacon is correlated from setup to setup, and thus divides out.

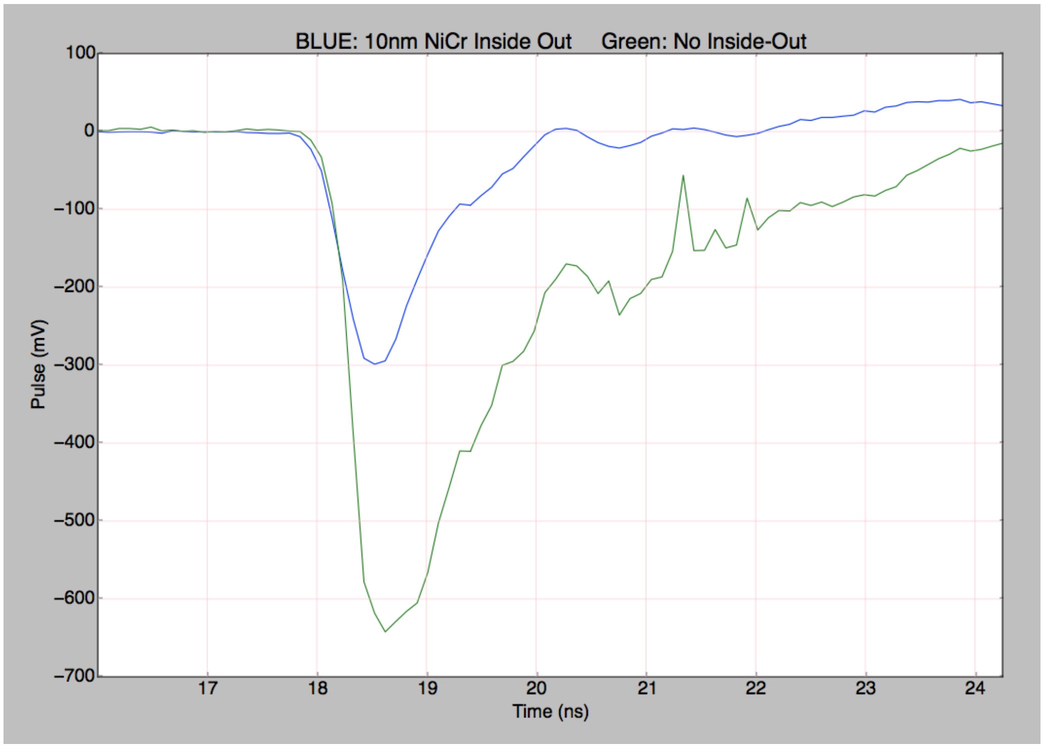

Figure 10: Two pulses aligned, one from an inside-out anode (blue) and another with direct strip-line measurement (green). The inside-out NiCr anode maintains about 40% of the amplitude, and the rise time is roughly the same as in the strip-line case. Notice that the ringing behavior between 20ns and 22ns is nearly identical between the two test anodes, demonstrating that noise sources from mutual capacitances in the system do not vary from setup to setup.

4.3. Rise time comparison

Another quantity which determines the timing resolution of an LAPPD is signal rise time. Here, the rise time is defined as the difference between the times where the signal passes 10% and 90% of its maximum.

Figure **??** shows that the rise time between direct and inside-out setups are nearly the same. The distribution is not entirely constant with applied high voltage due to electron multiplication effects in the MCPs [21]. The ratio between inside-out and direct is constant within errors. Here, the only errors shown are statistical, and they are on the order of 10% of the measured rise time.

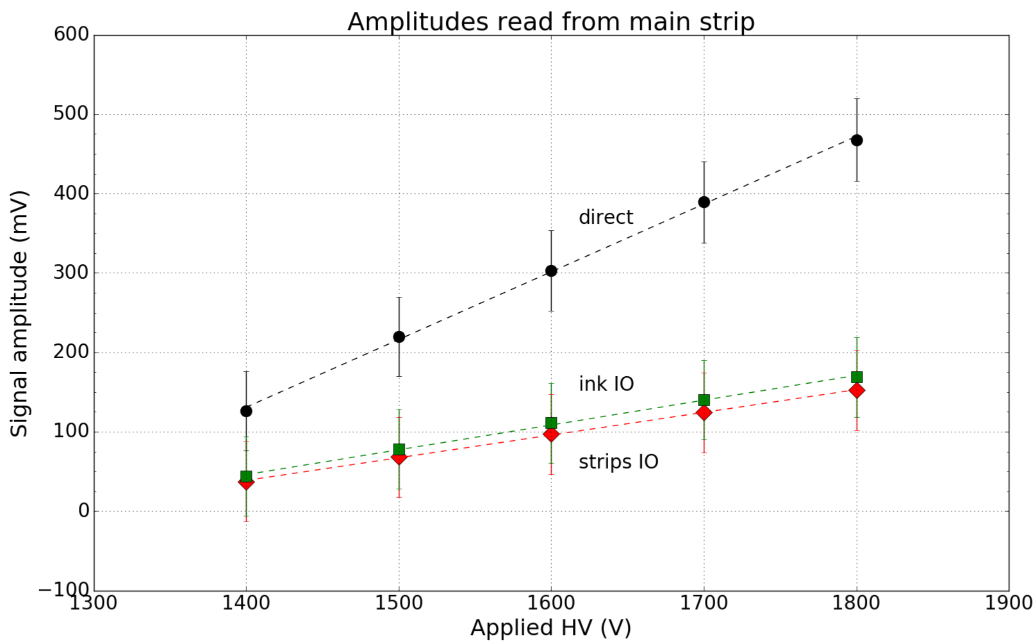

(a) This is a measurement of the average amplitude for pulses landing either directly on strip-lines or on an inside-out anode. The behavior of the amplitude as a function of high voltage is dependent on the physical properties of the micro-channel plates.

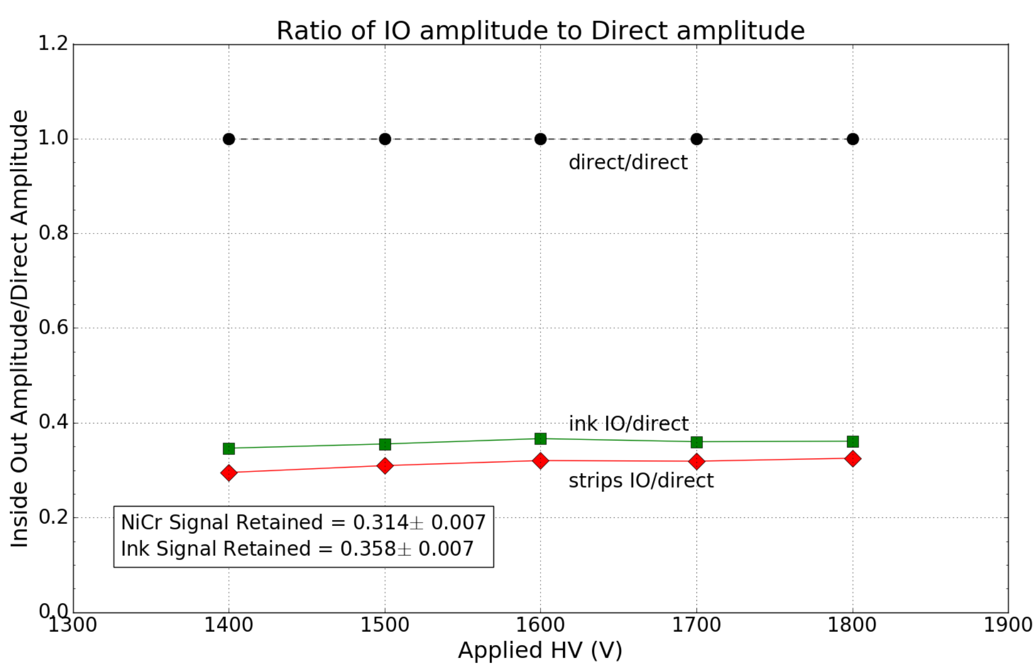

(b) The ratio between the amplitudes of the direct setp and the inside-out setup is approximately constant. In figure 11a, the slopes of the distributions differ due to effects in the MCPs. The ratio, however, is held constant, and is a measure of how much signal is retained when switching from first generation LAPPD to inside-out LAPPD. An average over all applied HV (with standard deviation) gives $35.8 \pm 0.7\%$ for the Ink inside-out sample, and $31.4 \pm 0.7\%$ for the NiCr inside-out sample.

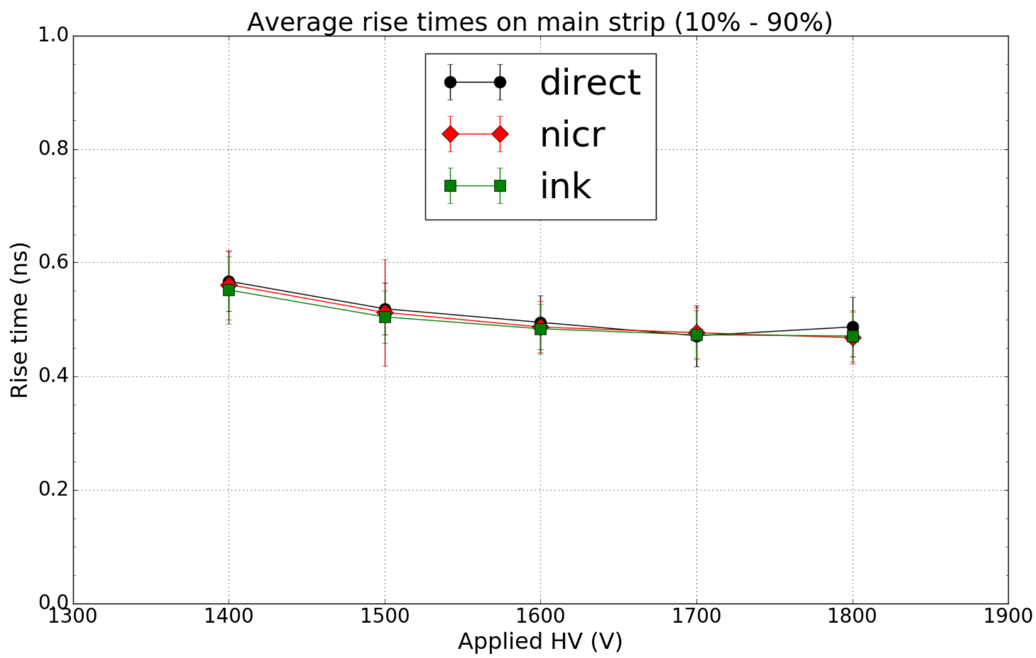

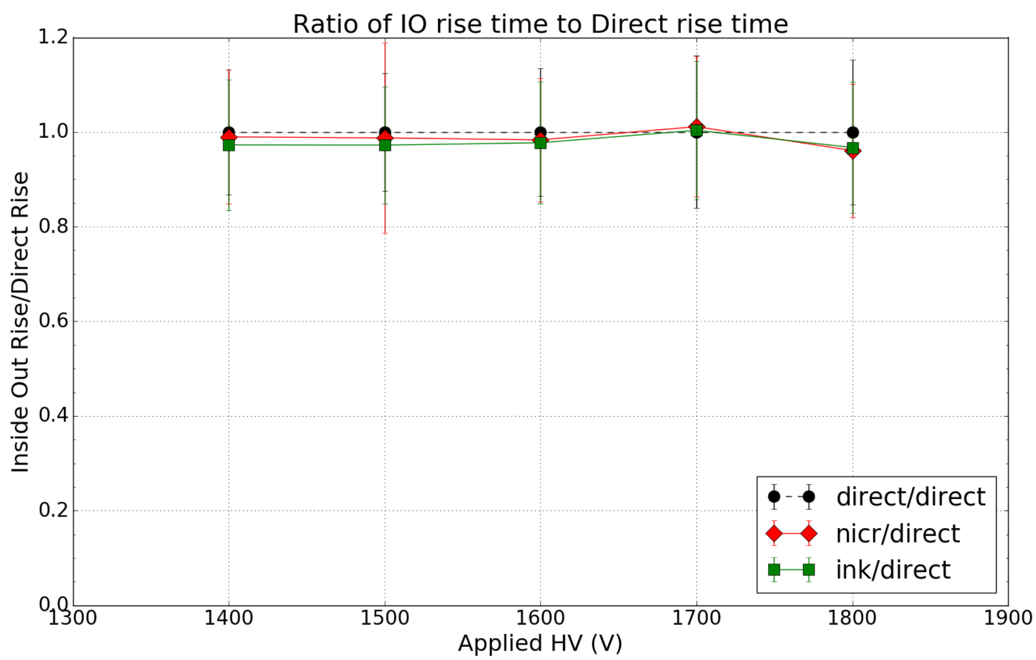

Figure 12: (TOP) Shows the average rise time in nanoseconds as a function of high voltage for all three test setups. The rise time is calculated by averaging all rise times after making cuts, and the standard deviation of this average is represented by the error bars. The result is that rise time does not change significantly when going from first generation LAPPD to inside-out LAPPD. This result is reinforced by the plot on the (BOTTOM), which shows a constant ratio between inside-out anodes and direct strip-lines.

5. Results and discussion

The plots above show that it is possible to couple MCP signals capacitively through a 3mm ceramic vacuum wall. The retained amplitude after capacitive coupling is calculated from the average over applied high voltages.

- 10nm NiCr, $\sim 100\Omega$ per square: $31.4 \pm 0.7\%$ signal amplitude retained
- 1000Ω per square resistive ink anode: $35.8 \pm 0.7\%$ signal amplitude retained

The 1000Ω per square ink anode retains $\sim 4\%$ more signal than the NiCr inside-out. This is within the systematic errors of the measurement. Therefore, a more resistive inside-out anode transmits a larger fraction of photo-signal. The two inside-out anodes differ by an order of magnitude in resistance, yet only a 4% increase in amplitude is measured. More inside-out samples must be tested in order to optimize signal transmission.

The rise time of MCP signals is roughly unchanged when switching to an inside-out anode. This measurement will need to be improved in order to make any conclusions about the timing characteristics of a second generation LAPPD.

6. Conclusion

By cutting manufacturing costs and simplifying the LAPPD design, a broader scope of physics applications will be able to afford and implement fast timing measurements. The second generation LAPPD introduces the inside-out anode, a thin metal ground plane that is internal to the vacuum volume.

This first test has shown that it is possible to capacitively couple internal LAPPD signals, through a ceramic vacuum wall, to an external strip-line readout board. The two inside-out anodes tested retained $31.4 \pm 0.7\%$ and $35.8 \pm 0.7\%$ of the signal, respectively for NiCr and resistive ink. No significant change in rise time was observed.

The goal of the LAPPD project is to allow a broad range of physics experiments to access smaller time scales. This result marks a significant step towards fabricating an affordable fast timing photo-detector.

7. Acknowledgments

We would like to thank Eric Oberla for having patience with us during a very busy time. With his help, we got past mistakes as we learned how to use the PSEC4 ASIC chips. We also thank Jeffrey DeFazio from Photonis for helping us diagnose and fix our Planacon photo-detectors which were essential for our measurements.

[1] Hamamatsu, *Photomultiplier Tubes, Basics and Applications*. See http://psec.uchicago.edu/links/pmt_handbook_complete.pdf

[2] See http://pdg.lbl.gov/

[3] Glenn R, Jocher, Matthew J. Wetstein, Bernhard Adams, Kurtis Nishimura, Shawn M. Usman. *Multiple-photon disambiguation on stripline-anode Micro-Channel Plates*. NIM A. Vol. 822, 21 June 2016, 25-33

[4] I. Angehel et. al. *Letter of Intent: The Accelerator Neutrino Neutron Interaction Experiment (ANNIE)*. See http://annie.fnal.gov/

[5] E. Oberla and H. Frisch, *The design and performance of a prototype water Cherenkov optical time-projection chamber*, to be published, Nucl. Instr. Meth., Jan. 2016

[6] B. Baller et. al. *Liquid Argon Time Projection Chamber Research and Development in the United States*. Mar 9 2014, arXiv: 1308.8166

[7] Minfang Yeh. Presentation: *Liquid Scintillator Timing Property* Neutrino and Nuclear Chemistry, BNL. Workshop December 15, 2015. See http://psec.uchicago.edu/workshops/PSEC4A/LiquidScintillatorTiming_MinfangYeh.pdf

[8] C. Aberle, A. Elagin, H.J. Frisch, M. Wetstein, L. Winslow. *Measuring directionality in double-beta decay and neutrino interactions with kiloton-scale scintillation detectors*. doi: 10.1088/1748-0221/9/06/P06012

[9] H. Kim, H. J. Frisch, C.-M. Kao, Q. Xie, C.-T. Chen, L. Zhou, F. Tang, W.W. Moses, W.S. Choong; *A Multi-Threshold Sampling ;Method for TOF PET Signal Processing*; Nuclear Instrument and Methods in Physics Research, A, 602, p. 618, 2009.

[10] H. Kim, H. J. Frisch, C.-T. Chen J.-F. Genat, F. Tang, W.W. Moses, W. S. Choong, and C.-M. Kao; *A Design of a PET Detector Using Micro-Channel Plate Photo-Multipliers with Transmission-Line Readout*; Nucl. Inst. and Meth. A622, p628 (2010)

[11] H. Kim, H. J. Frisch, C.-T. Chen J.-F. Genat, F. Tang, W.W. Moses, W. S. Choong, and C.-M. Kao; *A Prototype TOF PET Detector Module Using a Micro-Channel Plate Photomultiplier Tube with Waveform Sampling*; Nucl. Instr. and Meth. A662 (2012) 26-32

[12] Henry J. Frisch et al. *A Brief Technical History of the Large-Area Picosecond Photodetector (LAPPD) Collaboration* March 6, 2016. arXiv:1603.01843

[13] InnoSys, Inc.; *Multi-GHz RF-Microstrip Anodes for Micro-Channel Plate Photo-detectors*. Nov. 2013

[14] Hybrid-Tek, Inc. An Affiliate of Cetek. See http://www.hybrid-tek.com/

[15] Incom Inc. Charlton Mass. See http://www.incomusa.com/

[16] Todd Seiss et. al. A collaborative 335 project report within the University of Chicago LAPPD group. Soon to be posted online.

[17] Photonis, Planacon^{TM}; see the Planacon link at http://www.photonis.com/en/product/.

[18] Advanced Laser Diode Systems GmbH. See http://www.alsgmbh.de/

[19] E. Oberla, J.-F. Genat, H. Grabas, H. Frisch, K. Nishimura, and G Varner *A 15 GSa/s, 1.5 GHz Bandwidth Waveform Digitizing ASIC*, Nucl. Instr. Meth. A735, 21 Jan., 2014, 452;

[20] See the Table on factors that determine timing in *The Role of Analog Bandwidth and S/N in Timing* by S. Ritt in *The Factors that Limit Time Resolution in Photodetectors*; Workshop, University of Chicago, Chicago, IL; 28-29 April 2011; http://psec.uchicago.edu/workshops/. We note that with the resolution-determining factors of signal/noise having values of 1V, a sampling rate of 10 GS/sec, and an analog bandwidth of 3 GHz, the simple parametrization gives a resolution of 100 fsec. Of these, only the bandwidth has not been substantially exceeded, being 1.5 GHz.

[21] J.L. Wiza, Micro-channel Plate Detectors. Nuclear Instruments and Methods 162, 1979, pp 587-601